

Daisuke Miyazaki, Megumi Saito, Yoichi Sato, Katsushi Ikeuchi,
"Determining surface orientations of transparent objects based on polarization degrees in visible and
infrared wavelengths,"
Journal of Optical Society of America A,
Vol. 19, No. 4, pp.687-694, 2002.04

Determining Surface Orientations of Transparent Objects Based on Polarization Degrees in Visible and Infrared Wavelength

Daisuke Miyazaki

Institute of Industrial Science, The University of Tokyo, Tokyo

153-8505, Japan

miyazaki@cvl.iis.u-tokyo.ac.jp

Megumi Saito

Hewlett-Packard Japan, Ltd., Tokyo 168-8585, Japan

Yoichi Sato and Katsushi Ikeuchi

Institute of Industrial Science, The University of Tokyo, Tokyo

153-8505, Japan

{ysato, ki}@cvl.iis.u-tokyo.ac.jp

Techniques for modeling an object through observation are very important in object recognition and virtual reality. A wide variety of techniques have been developed for modeling objects with opaque surfaces, whereas less attention has been paid to objects with transparent surfaces. A transparent surface has only surface reflection; it has little body reflection. This paper presents a new method for obtaining surface orientations of transparent surfaces through analysis of the degree of polarization in surface reflection in visible and far infrared wavelengths, respectively. This parameter, the polarization degree of reflected light in the visible wavelength, is used for determining the surface orientation at a surface point. The polarization degree in visible wavelengths provides two solutions, and the proposed method uses the polarization degree in the far infrared wavelength to resolve this ambiguity. © 2001 Optical Society of America

OCIS codes: 110.3080, 110.6880, 120.4630, 120.6650, 260.5430, 330.7310

1. Introduction

Recently, techniques for modeling objects through observation have been extensively investigated. Such modeling has a wide area of applications, including virtual reality and object recognition. Geometry, one of the most important aspects of modeling, can be used to create a model based on measuring the shape of an object.

Many techniques to measure object shape have been developed in the field of optical engineering. These techniques can be classified into two categories: point and surface type. A point type method, such as a laser range sensor, measures object shape by projecting a spotlight, often a laser beam, over the object surface, and by measuring the returned timing or the returned direction.

A surface method, such as Moire topography, determines the shape of an object by projecting a planar light and measuring the interference of the light with the surface.

In addition, the computer vision community has extensively developed such techniques. Shape-from-shading, for example, analyzes shading information in an image with a reflectance map in order to relate image brightness to surface orientations. Photometric stereo obtains information from three images, taken from the same position, under three different illumination conditions. Binocular stereo and motion analysis use image differences in a series of images taken from different positions.

Most of these methods are, however, designed to obtain the shape of opaque surfaces. Namely, these techniques are based on analysis of the body reflection component of an object surface. Models of transparent objects, which have only surface reflection, cannot be created using these techniques. Few methods extant attempt to determine object shape through surface reflection.

With regard to surface reflection, Ikeuchi [1] proposed to determine the reflectance of a metal surface using photometric stereo. When exposed to three extended light sources, a metal surface generates different illumination distributions over the surface. The application of the photometric stereo method to these illumination distributions allows the shape of a metal surface to be determined. Nayar et. al. [2] extended the method by using continuous illumination distribution, referred to as a photometric sampler. Their method determines not only surface shape but also surface reflectance parameters. Sato et. al. [3] analyzed color images in a similar setting, and determined the shape and reflectance of shiny objects for computer graphics purposes, and Oren and Nayar [4] proposed a method using surface reflections and motion to determine surface shape.

Surface reflection can also be analyzed through the degree of polarization, as demonstrated by Kosikawa [5], who proposed to use the degree of polarization, employing polarized light sources to determine the shape of metal surfaces. Later, Koshikawa and Shirai [6] applied this method to the recognition of objects. Wolff [7] proposed to analyze the degree of polarization in visible light

for that same purpose. Wolff et. al. [8] indicated that the surface normal of the object surface is constrained by analyzing the polarization of the object; Rahmann [9] addressed the potential of recovering shape from polarization; and Jordan et. al. [10, 11] and Wolff et. al. [12] analyzed the degree of polarization in the infrared wavelength.

A transparent surface also has surface reflection components. Szeliski et. al. [13] analyzed the movement of surface reflection components on a transparent object, and separated surface reflection from background images. Schechner et. al. [14] proposed a method with which to determine only the surface reflection component, using the degree of polarization. That method also addressed the extraction of information about the orientation of transparent planes. For graphics applications, Zongker et. al. [15] developed a method with which to generate the appearance of a transparent object from a series of images taken under different background conditions. These methods, however, do not provide the shape information of a transparent object.

Saito et. al. [16, 17] employed the analysis of the degree of polarization and developed a method with which to measure the surface of a transparent object. Employing an extended light source originally developed by Nayar et. al. [2], they illuminated a transparent object and were able to obtain surface reflection components over the entire visible surface. Then, by measuring the degree of polarization, they determined surface orientations. Unfortunately, however, the degree provides two solutions corresponding to one polarization degree. Thus, the method can be applied to measuring a limited class of objects or to surface inspection where rough surface orientation is predetermined; it cannot be applied to a general class of objects.

In this paper, we propose to disambiguate these two solutions by introducing the polarization degree in the infrared wavelength. This new method first obtains the degree of polarization in the visible wavelength, which was likewise obtained in our earlier method. One polarization degree measured corresponds to two surface orientations. The polarization degree in the infrared wave-

length provides a single surface orientation to one polarization degree. Thus, by simultaneously measuring the degree in the infrared domain, we can uniquely determine the surface orientation. The measurement in the infrared wavelength cannot be used directly because the polarization ratio is relatively low in some areas, and it is therefore better to use this measurement solely for judgment purposes.

In Chapter 2, we present the background theory of polarization, and describe a method with which to obtain surface shape using the polarization degrees in both visible and infrared wavelengths. In Chapter 3, we describe the apparatus of this method and the experimental results. Chapter 4 concludes the paper.

2. Polarization and shape determination

A. Fresnel's equation

The light that reflects at the surface of most types of objects can be separated into two major components, surface reflection and body reflection. Incident light partly reflects at the surface and partly penetrates inside the object. The light that penetrates inside an opaque object randomly reflects at some of the pigments inside the object and is emitted into the air. The light that specularly reflects at the surface is called the surface reflection, and the light that is diffusely emitted into the air from inside the object is called the body reflection [18]. We focus only on transparent objects in this paper, analyzing surface reflection rather than body reflection.

In this section, we will briefly overview the basic equation of reflection and refraction [19]. In Figure 1, let us consider the case in which a light hits the interface surface between two materials, the refractive indices of which are denoted as n_1 and n_2 , respectively. Here we assume that the interface surface lies on the X-Y plane without loss of generality. One part of the light is reflected at the interface surface, while another part penetrates the surface and is refracted when entering

the second material. Because we assume that both materials are transparent, we can neglect the component to be absorbed. We denote the incident, reflected, and refracted light as the subscripts a , r , and t , respectively, and identify the parallel and perpendicular components to the X-Z plane as p and s , respectively. The incident, reflecting, and transmitting angles are defined as ϕ_1 , ϕ_1' , and ϕ_2 , respectively, as shown in Figure 1. Given that the incident and reflected light pass through the same materials, $\phi_1 = \phi_1'$, we can define the parallel and perpendicular reflectance ratios, F_p and F_s , respectively, as

$$\begin{aligned} F_p &= \frac{I_{rp}}{I_{ap}} = \frac{\tan^2(\phi_1 - \phi_2)}{\tan^2(\phi_1 + \phi_2)} \\ F_s &= \frac{I_{rs}}{I_{as}} = \frac{\sin^2(\phi_1 - \phi_2)}{\sin^2(\phi_1 + \phi_2)} \end{aligned} \quad (1)$$

where I_{ap} is the component parallel to the X-Z plane of the incident light, and I_{rp} is that of the reflected light. I_{as} is the component perpendicular to the X-Z plane of the incident light, and I_{rs} is that of the reflected light. From the above equation, an incident angle to make $F_p = 0$ can be obtained. This incident angle is referred to as the Brewster angle, ϕ_B . The Brewster angle is obtained by substituting $\phi_1 + \phi_2 = \pi/2$ (namely, $F_p = 0$) into Snell's equation, $n_1 \sin \phi_1 = n_2 \sin \phi_2$, as

$$\tan \phi_B = \frac{n_2}{n_1}. \quad (2)$$

B. Determining surface orientations using polarization

An interface surface of a transparent object causes little diffuse reflection or absorption; under the condition of the reflected light, the incident and reflecting angles are same. Thus, once the reflecting angle and the orientation of the plane of incidence are known, we can determine the surface orientation with respect to the viewer, as shown in Figure 2. Here the plane of incidence is the one on which the light source, surface normal, and the viewer vectors lie. We will denote the direction of the plane of incidence and the reflecting angle as θ and ϕ , respectively. We will

determine these two angles using the degree of polarization of reflected light.

Generally speaking, natural light is unpolarized; it oscillates in all directions on the plane of oscillation, which is perpendicular to the path of the light. Natural light, however, becomes polarized once it goes through a polarization material or is reflected on a surface. We will measure the degree of polarization for this purpose.

As shown in Equation (1), the intensity varies depending on the direction on the plane of oscillation, and therefore a difference can be observed when the polarization filter is rotated in front of a CCD camera. The variance is described as a sinusoidal function of rotation angles. We will denote the maximum and minimum brightness in the observed intensities as I_{\max} and I_{\min} . Given that the sum of the maximum and minimum brightness is the total brightness of the reflected light, I_{specular} ,

$$I_{\max} = \frac{F_s}{F_p + F_s} I_{\text{specular}}, \quad I_{\min} = \frac{F_p}{F_p + F_s} I_{\text{specular}}. \quad (3)$$

By this equation, the direction parallel to the plane of incidence provides the minimum brightness I_{\min} . Namely, by measuring the angle to give the minimum brightness, we can determine the direction of the plane of incidence, θ . There are two possible directions of the plane of incidence, θ_1 and θ_2 , which are definable as $\theta_2 = \theta_1 + \pi$. We assume the surface as a convex shape, and we avoid this ambiguity.

The definition of the degree of polarization is as follows:

$$\rho = \frac{I_{\max} - I_{\min}}{I_{\max} + I_{\min}}. \quad (4)$$

The degree of polarization is 0 when the light is unpolarized, whereas it is 1 when the light is linearly polarized. The linearly polarized light is observed when the parallel component becomes 0. This occurs when the incident angle and the reflecting angle are at the Brewster angle.

By substituting Equation (3) and (1) into Equation (4) with Snell's law, we can represent the

degree of polarization, ρ , as

$$\rho = \frac{2 \sin \phi \tan \phi \sqrt{n^2 - \sin^2 \phi}}{n^2 - \sin^2 \phi + \sin^2 \phi \tan^2 \phi}. \quad (5)$$

The degree of polarization is a function of the refractive index, n , and the incident angle, ϕ . Thus, by obtaining the degree of polarization from the data, we can determine the incident angle, ϕ , given the refractive index n .

Figure 3 shows the relation between the degree of polarization and the incident angle. Here, the horizontal and vertical axes denote the incident angle and the degree of polarization, respectively. We can obtain the incident angle from the observed degree of polarization even if we do not know the intensity of the light source. The function has an extreme at the Brewster angle. From this function, an observed degree of polarization provides two possible incident angles, except at the Brewster angle. It is necessary to have a method to resolve this ambiguity. In this paper, we propose to solve this problem by considering the polarization of far infrared light.

C. Thermal radiation

Heat energy can propagate through space. This phenomenon is referred to as heat propagation. A blackbody can completely absorb the heat energy radiated. According to Kirchhoff's law, the ratio between radiant and incoming heat energy is independent of the object and dependent only on the temperature of the object. A blackbody, which completely absorbs energy, can also radiate more energy than any other objects at the same temperature.

From the Stephan-Boltzman law, radiation energy, W , from the blackbody at the temperature T is

$$W = \sigma T^4 \quad (6)$$

where σ is the Stephan-Boltzmann coefficient and $\sigma = 5.67 \times 10^{-8}$ [W/m²·K⁴]. Given that any object has a positive temperature, any object should radiate energy.

A blackbody has an energy distribution, as shown in Figure 4. From the figure, it is apparent that the extremes of distributions shift along the temperature increment, and in the area of room temperature, they exist in the infrared region. Thus, it is appropriate to employ infrared measurement for measuring the radiation energy of a blackbody at room temperature.

In next two sections, we will derive the polarization degree in infrared light, by two respective approaches. In Section **D.** the polarization degree is derived by using Kirchhoff's law, and in Section **E.** the polarization degree is derived by considering the light emitted from inside the objects. As a result, both of the derived polarization degrees will be the same equation.

Glass is transparent in visible light, though it is somewhat translucent (or maybe opaque?) in infrared light; that is, glass is more likely to absorb infrared light than visible light. First, we will describe the unified theory of the polarization in infrared light, which does not depend on whether the object is transparent, translucent, or opaque.

To actualize this idea, let us assume that in a sense, all objects can be considered opaque; the light that hits the interface surface of objects can only reflect or be absorbed. The light that transmits into a transparent object will then be called the light that is absorbed into it. The light transmitted into a transparent object escapes into the air somewhere from the surface of the object. Let us say that such escaped light is the light (thermally) emitted from the object.

This assumption that all objects can be considered opaque is used in Section **D.**. This assumption holds when the corollary is in thermal equilibrium, given that all light is expected to have the same amount of energy and radiate in all directions.

D. Kirchhoff's law

By considering the state when the corollary is in thermal equilibrium, and by using Kirchhoff's law, we can explain the polarization of thermal radiation[10, 11, 12, 20, 21].

A typical object emits a lower amount of radiation energy than that emitted from a blackbody.

The ratio of the amount of radiation energy of a typical object in relation to that from a blackbody is referred to as the emissivity, and denoted as ε .

Let us assume that infrared light strikes a smooth surface. Its parallel and perpendicular intensity to the plane of incidence are denoted as I_{ap} and I_{as} , respectively. When the infrared light strikes a surface with the incident angle ϕ , the intensity of parallel and perpendicular components of reflected light are given as $F_p I_{ap}$ and $F_s I_{as}$, respectively.

From the law of the conservation of energy, the difference between the incoming and reflected intensities, $(1 - F_p)I_{ap}$ and $(1 - F_s)I_{as}$, are the amount of energy absorbed to the body. By denoting this ratio as absorptance α , since Kirchoff's law provides $\varepsilon = \alpha$, we obtain

$$\begin{aligned}\varepsilon_p(T, \lambda, \phi) &= 1 - F_p \\ \varepsilon_s(T, \lambda, \phi) &= 1 - F_s.\end{aligned}\tag{7}$$

Let us denote the intensity of thermal radiation from the perfectly blackbody as W . Then, the intensity of thermal radiation from our object is εW , and its polarization can be written by using Equation (7):

$$\begin{aligned}\rho_{\text{IR}} &= \frac{I_{\text{max}} - I_{\text{min}}}{I_{\text{max}} + I_{\text{min}}} = \frac{\varepsilon_p W - \varepsilon_s W}{\varepsilon_p W + \varepsilon_s W} \\ &= \frac{F_s - F_p}{2 - F_p - F_s}\end{aligned}\tag{8}$$

where ρ_{IR} is the polarization degree in infrared light. We use the different notation to distinguish this condition from that in the visible light. By substituting Equation (1) for Equation (8), we can derive the relation between the polarization ratio, ρ_{IR} , and the emitting angle, ϕ .

E. Light emitted from inside the object

Let us explain the polarization phenomenon of thermal radiation by considering the light emitted from inside the object [22]. Thermal radiation emitted from inside the object is transmitted through the interface surface and radiated into the air.

Material 1 will be the object and material 2 will be the air, as shown in Figure 1. In this case, $\phi_2 > \phi_1$. We denote the refractive index of material 1 as n_1 and that of material 2 as n_2 . Thus, the refractive index of the object relative to the air will be $n = n_1/n_2$. ϕ_2 is the emitting angle, and we will derive the polarization degree as a function of $\phi = \phi_2$.

We can define the parallel and perpendicular intensity ratios of transmission, T_p and T_s , as

$$\begin{aligned} T_p &= \frac{I_{tp}}{I_{ap}} = \frac{\sin 2\phi_1 \sin 2\phi_2}{\sin^2(\phi_1 + \phi_2) \cos^2(\phi_1 - \phi_2)} \\ T_s &= \frac{I_{ts}}{I_{as}} = \frac{\sin 2\phi_1 \sin 2\phi_2}{\sin^2(\phi_1 + \phi_2)} \end{aligned} \quad (9)$$

where I_{tp} is the component parallel to the X-Z plane of the transmitting light, and I_{ts} is the component perpendicular to the X-Z plane of the transmitting light. Thus, I_{\max} and I_{\min} will be written by using the total energy of the emitted light, W , as

$$I_{\max} = \frac{T_p}{T_p + T_s} W, \quad I_{\min} = \frac{T_s}{T_p + T_s} W. \quad (10)$$

By substituting Equation (10) and (9) into Equation (4) with Snell's law, we can represent the degree of polarization of thermal radiation ρ_{IR} as

$$\begin{aligned} \rho_{\text{IR}} &= \frac{I_{\max} - I_{\min}}{I_{\max} + I_{\min}} = \frac{T_p - T_s}{T_p + T_s} = \frac{s}{2 - s} \\ s &= \sin^2 \phi \left(1 + \frac{1}{n^2} - \frac{2}{n^2} \sin^2 \phi - \frac{2}{n} \sqrt{(1 - \sin^2 \phi) \left(1 - \frac{1}{n^2} \sin^2 \phi \right)} \right). \end{aligned} \quad (11)$$

F. Graph of polarization degree in infrared light

$F_p + T_p = 1$ and $F_s + T_s = 1$ holds, thus the resulting ρ_{IR} in both Section **D**. (Equation (8)) and Section **E**. (Equation (11)) are the same. This is because both explanations deal with the same phenomenon, though the approach is different; one is based on the energy conservation law (Kirchhoff's law), the other on the mechanism of the phenomenon.

Figure 5(a) shows the relation between the polarization ratio, ρ_{IR} , and the emitting angle, ϕ .

The refractive index of the graph shown in Figure 5(a) is 1.5. Because the refractive index is affected by the wavelength, the refractive index of infrared light is slightly different from that of visible light. For example, the refractive index of glass is approximately 1.52 when the wavelength is approximately 500nm (visible light), and the refractive index of glass is approximately 1.49 when the wavelength is approximately $2\mu\text{m}$ (infrared light). We use the same refractive index in infrared light as that in visible light because the difference is negligible.

As shown in Figure 5(a), the relation is a one-valued function; there is a one-to-one correspondence between the ratio and the emitting angle. Thus, once we measure the ratio in an infrared light, we can uniquely determine the emitting angle. For the sake of comparison, Figure 5(b) represents the visible light condition. In this function, as mentioned, one polarization ratio corresponds to two emitting angles.

Unfortunately, however, the ratio in emitted infrared light is much smaller than that in reflected visible light; at the maximum, around an emitting angle of 90 degrees, it is still 40%. In the smaller area, the ratio is smaller than 10%. In order to obtain such a smaller ratio, we are required to measure I_{max} and I_{min} precisely. It is impractical to perform such a highly accurate measurement using an ordinary CCD camera with a 256 gray level.

In order to overcome this difficulty, we propose to use both visible and infrared light. By using visible light, we can achieve a highly accurate measurement with ambiguity. By using the infrared light, we discriminate between the two sides. First we determine the polarization ratio in the infrared region at the Brewster angle. Using this ratio as the threshold value, we can determine to which side, with respect to the Brewster angle, the emitting angle belongs, as indicated by the dotted line in Figure 5.

3. Determining surface orientation of transparent object

A. Apparatus for visible light measurement

Figure 6(a) shows the apparatus for visible light measurement. As a light source, we employ a spherical diffuser illuminated from point light sources. This spherical diffuser becomes a secondary light source and illuminates an object that is located at the center of the sphere from all directions. Because we determine surface orientations using only surface reflection and the surface reflection occurs only when the emitting and incident angles are the same, it is necessary to illuminate an object from all directions in order to observe surface reflections over the entire object surface.

We use three 300W incandescent light bulbs as the point sources, located circularly and at 120 degrees apart. The spherical diffuser is made of plastic and its diameter is 40 cm. The object, as mentioned above, is located at the center of the sphere, and is illuminated by this spherical diffuser, which works as an unpolarized spherical light source. This object is observed through a small hole at the top of the sphere by a black and white CCD camera. A polarization filter is mounted between the hole and the TV camera.

B. Apparatus for infrared light measurement

Figure 6(b) shows the apparatus for the infrared light. Given that the infrared light is thermal radiation from a body and is not a reflection component, we do not use any light source. Any object emits infrared light. However, at room temperature, the amount of infrared light emitted from the object in 3-5 μm is relatively small, and contains infrared light emitted from the air. This makes the measurement of I_{max} and I_{min} very sensitive to noise. Thus, we increase the temperature of the object to 30-40 degrees Celsius, and subtract that from the air to obtain the amount of infrared light emitted solely from the object.

In order to increase the temperature of the object, we use a hair dryer to blow heated air

over it. We also employ an infrared filter and an IR-CCD camera in 3-5 μm . Our IR-CCD camera determines an appropriate gain in order to map the temperature range into a 256 gray level. Thus, a measured intensity is converted to a temperature. In order to determine the polarization ratio, we convert the measured temperature into intensity using Equation (6).

C. Experimental method

Because a transparent object reflects and transmits light, the observed intensity in visible light measurement is the combination of the light reflected at the surface and the light transmitted from behind the object. We put the object on a black pipe to block the light from behind the object. We should observe only the light reflected directly on the surface and originating from the light source, though the light reflects and transmits randomly through the object. The shape of the object is not known a priori, so we cannot exactly estimate such internal reflection. We assume that any light not directly reflected from the surface is relatively small, and that we observe only the light reflected directly at the surface.

In visible light measurement, by rotating a polarization filter, we obtain a sequence of images of an object. We measure from 0 degrees through 180 degrees at 5 degree intervals. From this process we obtain 36 images.

At each pixel of the 36 images, we observe variance of intensity and determine the maximum and minimum intensities, I_{max} and I_{min} . Because those measurements occur at 5 degree intervals, it is difficult to obtain the exact maximum and minimum values. By using the non-linear least square minimization, we fit a sinusoidal curve to those obtained measurements, then determine the maximum and minimum values. From those values, we determine two possible surface orientations using the algorithm.

For the infrared measurement, we heat the object to a temperature of 30-40 degrees Celsius by using the hair dryer for a certain period. Once equilibrium in the heat exchange is achieved, we

use the same procedure, rotating the polarization filters and obtaining a sequence of images, as we did in the visible light measurement. Here, the maximum and minimum correspond to T_{\max} and T_{\min} ; we convert them to I_{\max} and I_{\min} as appropriate, then obtain the polarization degree.

At the third step, we compare the measurements in infrared and visible light at each pixel. For alignment, we use two calibration points around the object; by extracting these two points in both image sequences, we can align the two measurements. At each pixel, measurement in visible light provides two solutions. Then, from the polarization degree in infrared measurement, we can choose one of the solutions; it is determined whether the obtained polarization degree in infrared light is smaller or larger than the infrared polarization degree at the Brewster's angle, ρ_{IR}^* .

D. Experiments using a spherical object

In order to determine the accuracy of the system, we use an acrylic sphere having a refractive index of 1.5 and a diameter of 5cm. Figure 7 shows the error characteristics from the observed measurement. The horizontal axis is the emitting angle and the vertical axis denotes the measurement errors. In the figure, the dotted straight line denotes the case without any measurement errors.

From this experiment, except around the area of small angles, the measurement error is small and we can achieve high accuracy in measurement.

One of the reasons for the relatively noisy data around the smaller angles is that the spherical diffuser has a hole in its top portion, and the object does not receive light from that area. Another reason is that the derivative of the degree of polarization is close to zero where the incident angle is near 0° , and is less stable for determining the incident angle from the degree of polarization.

E. Experiments using a shellfish-shaped object

In order to demonstrate the applicability of our system to an object of general shape, we determined the shape of the object shown in Figure 8(a). The shellfish-shaped object is made of acrylic and its

refractive index is 1.5. Figure 8(b) shows the obtained shape of the object. Here the system provides the distribution of surface orientations. From this obtained distribution, a relaxation algorithm [23] converts the orientation distribution into a shape corresponding to that of the object.

Figure 8(b) recovers the original shape. Notably, the area of steeper angles (i.e., those larger than the Brewster angle) provides better recovery results. At the boundary, the shape is a bit noisy. At that region, the polarization ratio is almost zero, and it is difficult to determine this value.

4. Conclusion

This paper proposes a method by which to determine the shape of a transparent object using polarization. Surface orientations are determined using the polarizations in visible light. Because an algorithm using visible light provides ambiguities, polarization in infrared is then employed. The thermal radiation, which also has characteristics of polarization, can be observed as infrared light. This polarization is a one-valued function; measuring polarization ratio in infrared provides the emitting angle. However, the ratio is relatively low, and in some cases it is difficult to determine the ratio precisely. Thus, we propose to use polarization in both visible and infrared light.

We have implemented the proposed method, and demonstrated its ability to determine the shape of a transparent object. First, by using a spherical acrylic object, we determined the accuracy of the method in the visible light region, and demonstrated its effectiveness. Then, using an object of general shape, we demonstrated the ability of the system to determine the shapes of complex objects.

References

1. K. Ikeuchi, "Determining surface orientations of specular surfaces by using the photometric stereo method," *IEEE Trans. Patt. Anal. Mach. Intell.* **3**, 661-669 (1981).
2. S. K. Nayar, K. Ikeuchi, and T. Kanade, "Determining shape and reflectance of hybrid surface by photometric sampling," *IEEE Trans. Rob. Auto.* **6**, 418-431 (1990).
3. Y. Sato, M. D. Wheeler, and K. Ikeuchi, "Object shape and reflectance modeling from observation," in *Proc. SIGGRAPH 97*, (Addison Wesley, Boston, MA, 1997), pp.379-387.
4. M. Oren, and S. K. Nayar, "A theory of specular surface geometry," *International Journal of Computer Vision* **24** (2), 105-124 (1997).
5. K. Koshikawa, "A polarimetric approach to shape understanding of glossy objects," in *Proc. Int. Joint Conf. Artificial Intelligence*, (Morgan Kaufmann, Los Altos, CA, 1979), pp.493-495.
6. K. Koshikawa, and Y. Shirai, "A model-based recognition of glossy objects using their polarimetric properties," *Advanced Robotics* **2** (2), 137-147 (1987).
7. L. B. Wolff, "Polarization-based material classification from specular reflection," in *IEEE Trans. Patt. Anal. Mach. Intell.* **12** (11), 1059-1071 (1990).
8. L. B. Wolff and T. E. Boult, "Constraining object features using a polarization reflectance model," *IEEE Trans. Patt. Anal. Mach. Intell.* **13** (7), 635-657 (1991).
9. S. Rahmann, "Polarization images: a geometric interpretation of shape analysis," in *Proc. Int. Conf. on Pattern Recognition*, (IEEE Computer Society Press, Los Alamitos, CA, 2000), pp.542-546.

10. D. L. Jordan and G. D. Lewis, "Measurements of the effect of surface roughness on the polarization state of thermally emitted radiation," *Opt. lett.*, **19**, 692-694, (1994).
11. D. L. Jordan, G. D. Lewis, and E. Jakeman, "Emission polarization of roughened glass and aluminum surfaces," *Appl. Opt.*, **35**, 3583-3590, (1996).
12. L. B. Wolff, A. Lundberg, and R. Tang, "Image understanding from thermal emission polarization," in *Proc. IEEE Conf. Computer Vision and Pattern Recognition*, (IEEE Computer Society Press, Los Alamitos, CA, 1998), pp.625-631.
13. R. Szeliski, S. Avidan, and P. Anandan, "Layer extraction from multiple images containing reflections and transparency," in *Proc. IEEE Conf. Computer Vision and Pattern Recognition*, (IEEE Computer Society Press, Los Alamitos, CA, 2000), pp.246-253.
14. Y. Schechner, J. Shamir, and N. Kiryuati, "Polarization-based decorrelation of transparent layers: the inclination angle of an invisible surface," in *Proc. IEEE Int. Conf. Computer Vision*, (IEEE Computer Society Press, Los Alamitos, CA, 1999), pp.814-819.
15. D. E. Zongker, D. M. Warner, B. Curless, and D. H. Salesin, "Environmental matting and compositing," in *Proc. SIGGRAPH 99*, (Addison Wesley, Boston, MA, 1999), pp.205-214.
16. M. Saito, Y. Sato, K. Ikeuchi, and H. Kashiwagi, "Measurement of surface orientations of transparent objects using polarization in highlight," in *Proc. IEEE Conf. Computer Vision and Pattern Recognition*, (IEEE Computer Society Press, Los Alamitos, CA, 1999), pp.381-386.
17. M. Saito, Y. Sato, K. Ikeuchi, and H. Kashiwagi, "Measurement of surface orientations of transparent objects by use of polarization in highlight," *J. Opt Soc. Am. A* **16** (9), 2286-2293 (1999).

18. K. E. Torrance and E. M. Sparrow, "Theory for off-specular reflection from roughened surfaces," *J. Opt. Soc. Am.* **57** (9), 1105-1114 (1967).
19. M. Born, and E. Wolf, *Principles of Optics*, (Pergamon, New York, 1959).
20. F. E. Nicodemus, "Directional reflectance and emissivity of an opaque surface," *Appl. Opt.*, **4**, 767-773, (1965).
21. F. E. Nicodemus, "Reflectance nomenclature and directional reflectance and emissivity," *Appl. Opt.*, **9**, 1474-1475, (1970).
22. O. Sandus, "A review of emission polarization," *Appl. Opt.*, **4** (12), 1634-1642 (1965).
23. K. Ikeuchi, "Reconstructing a depth map from intensity maps," in *Proc. Int. Conf. on Pattern Recognition*, (IEEE Computer Society Press, Los Alamitos, CA, 1984), pp.736-738.

List of Figures

1	The Fresnel reflection	21
2	Surface normal of object	22
3	Relation between the degree of polarization and the incident angle ($n = 1.5$)	23
4	Energy distribution of blackbody	24
5	Polarization degree of (a)infrared light ($n = 1.5$), and (b)visible light ($n = 1.5$) .	25
6	Experimental setup	26
7	Error characteristics of the spherical object	27
8	The resulting shape of the shellfish-shaped object	28

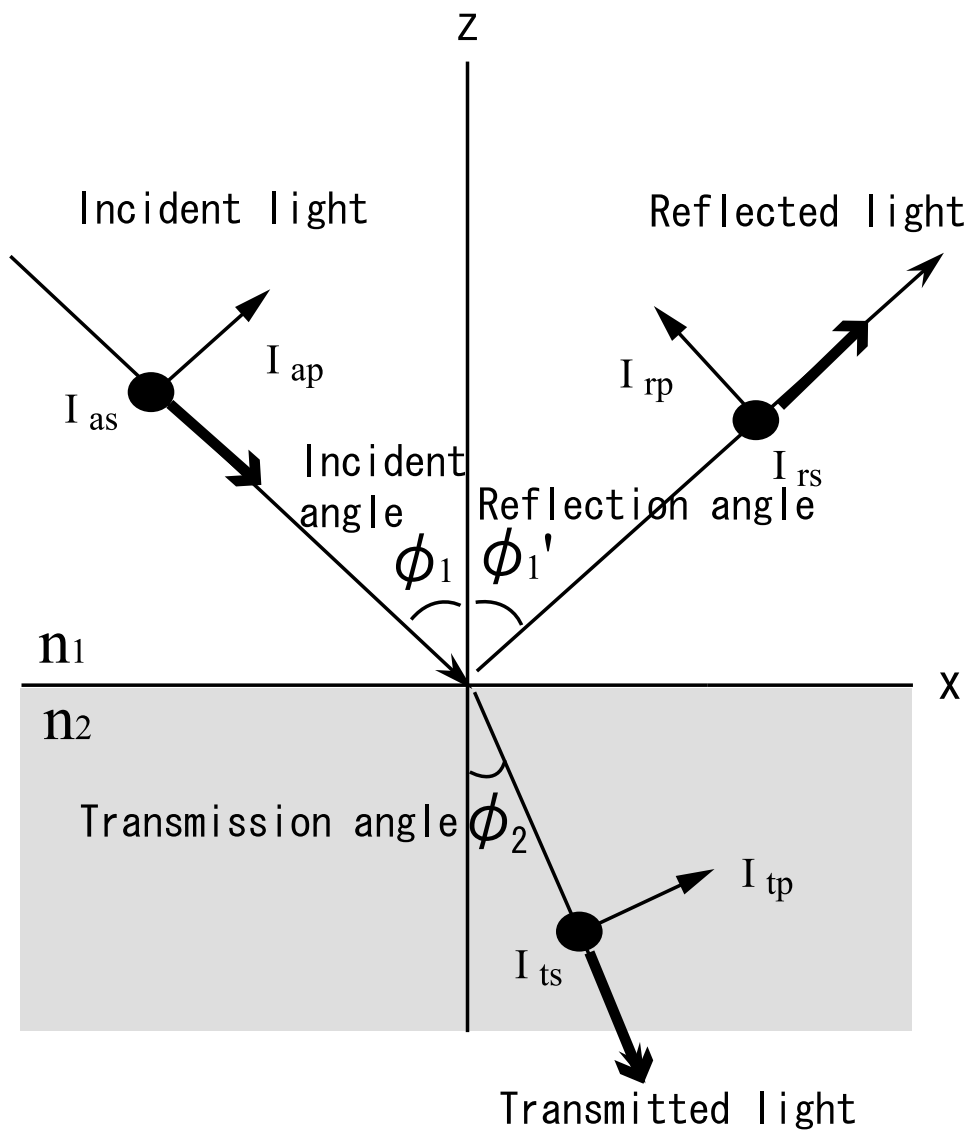


Fig. 1. The Fresnel reflection

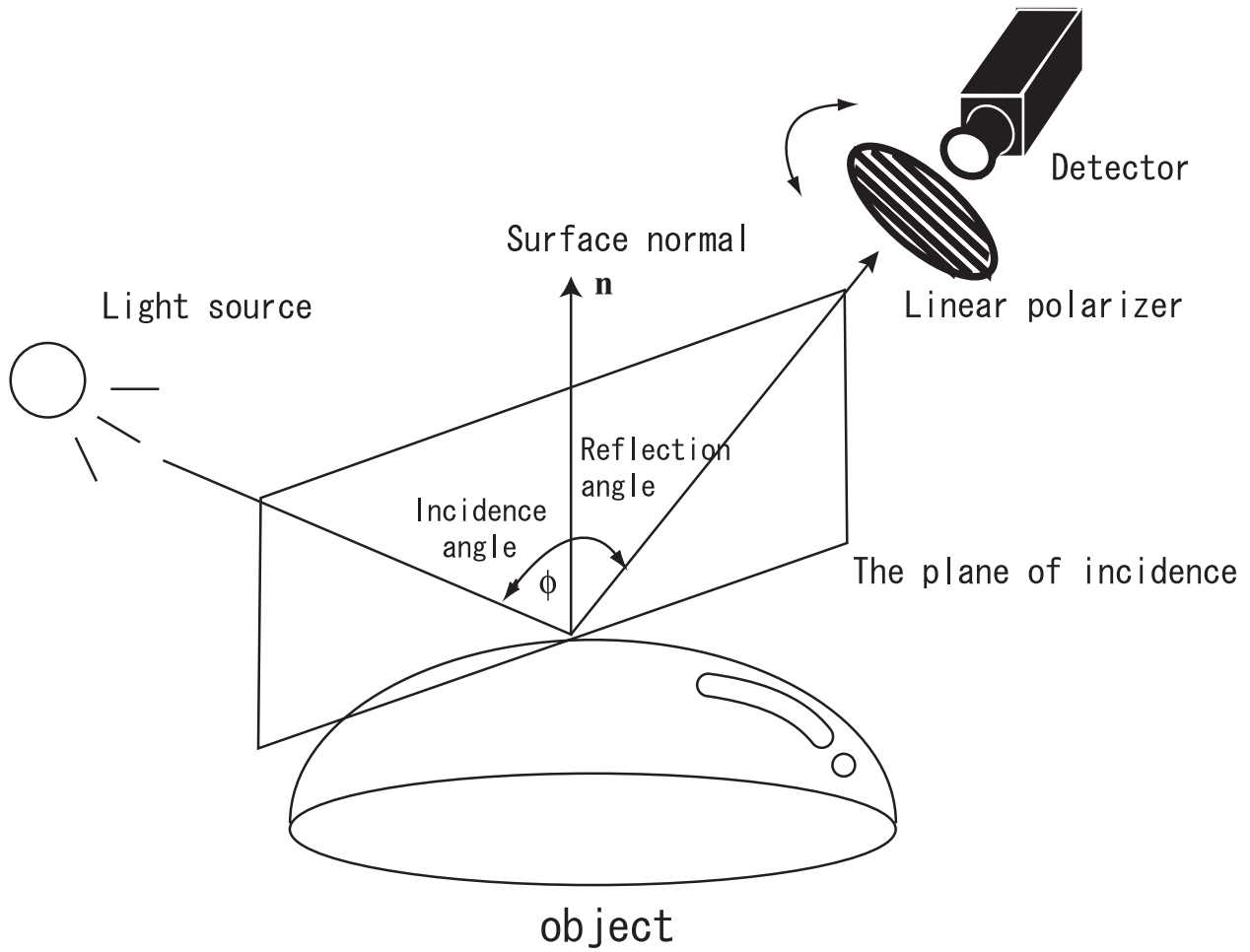


Fig. 2. Surface normal of object

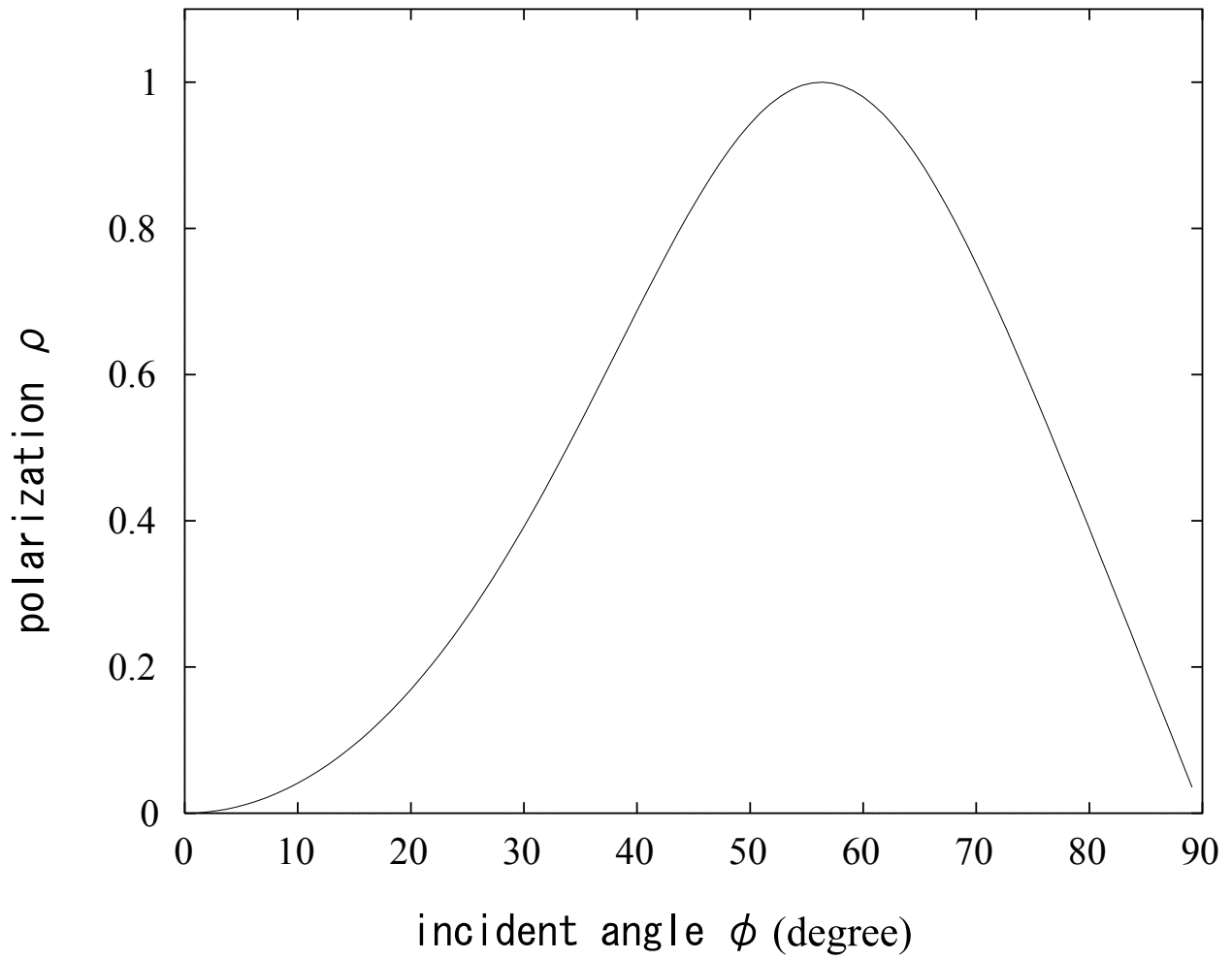


Fig. 3. Relation between the degree of polarization and the incident angle ($n = 1.5$)

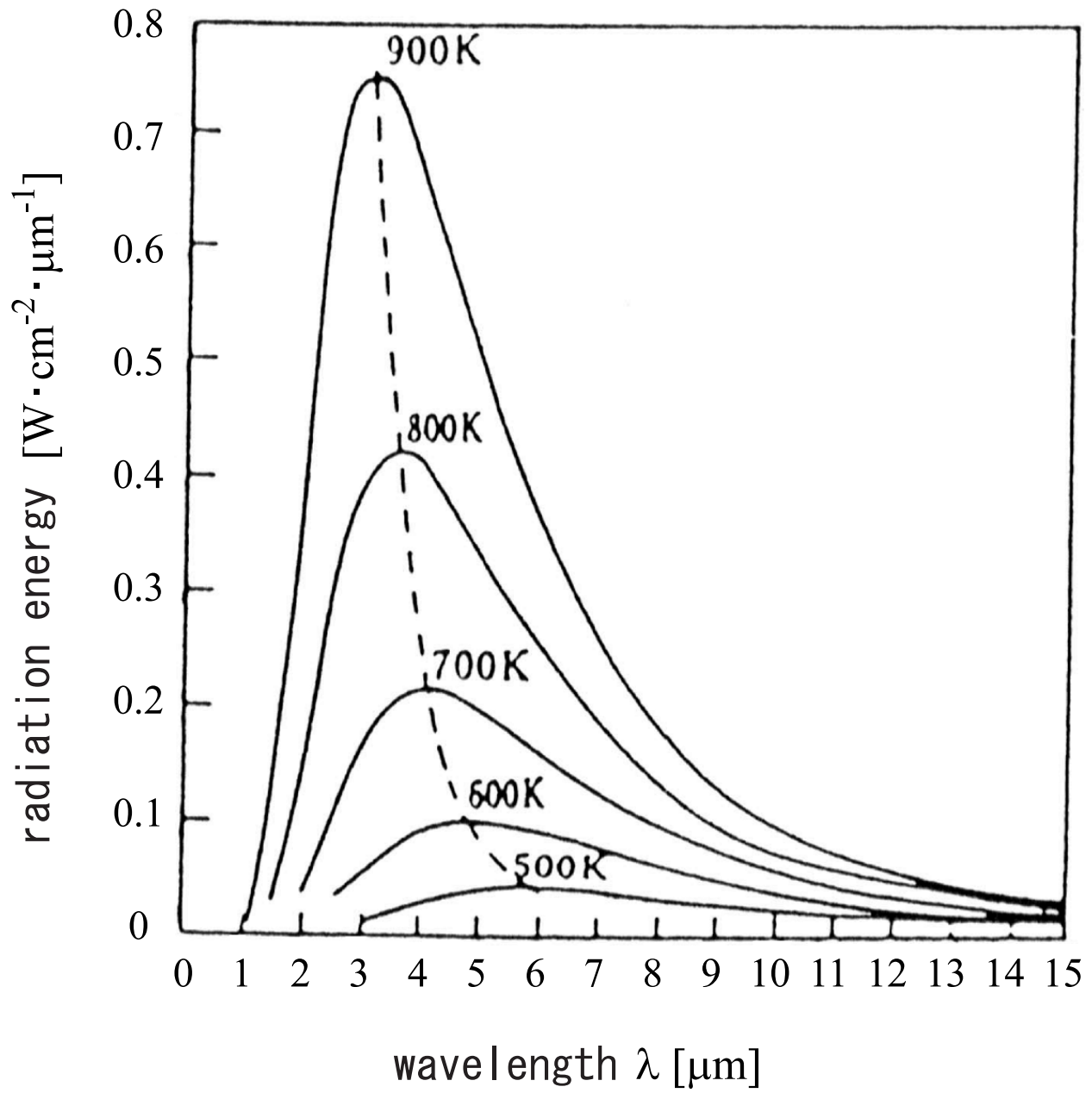


Fig. 4. Energy distribution of blackbody

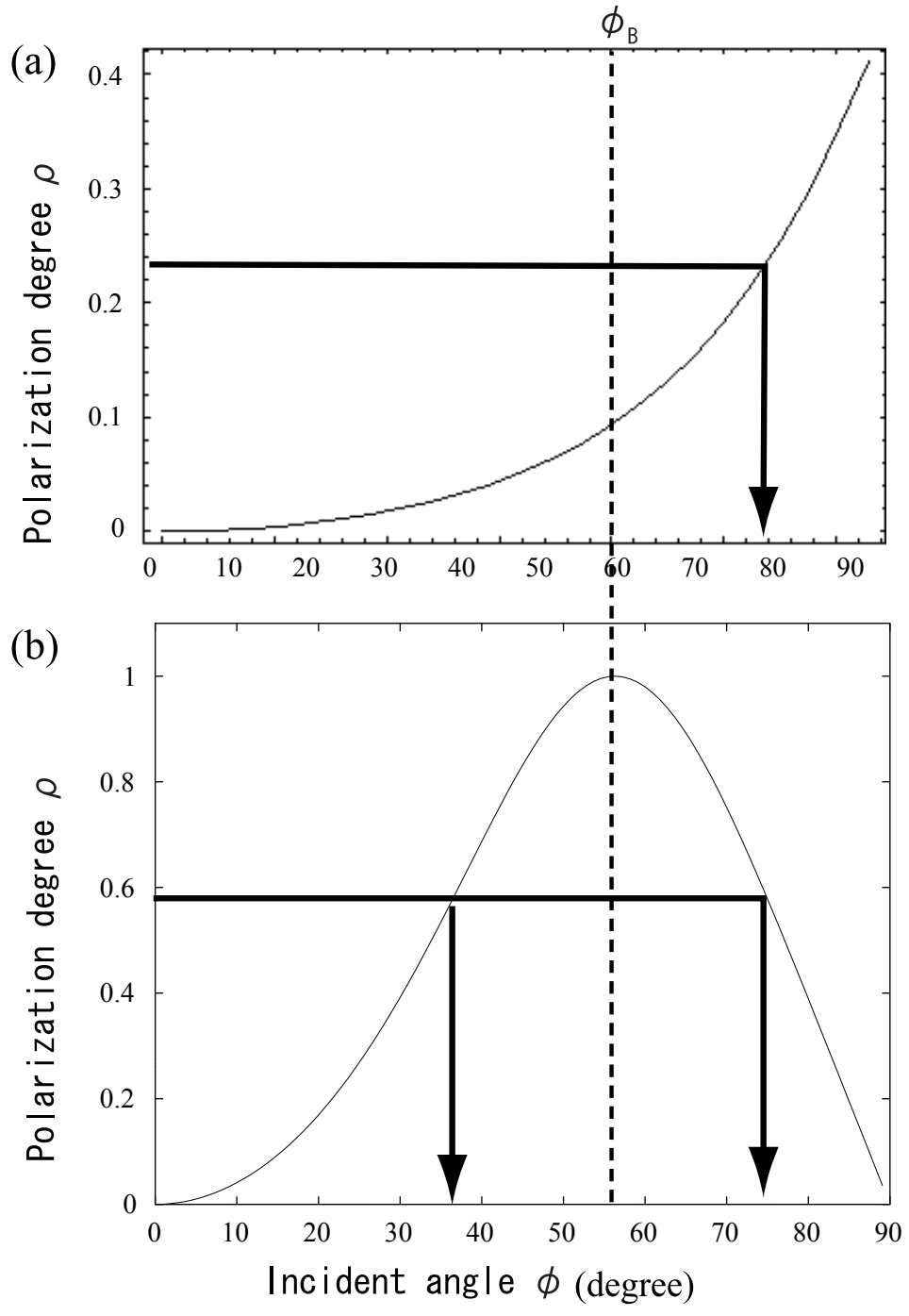
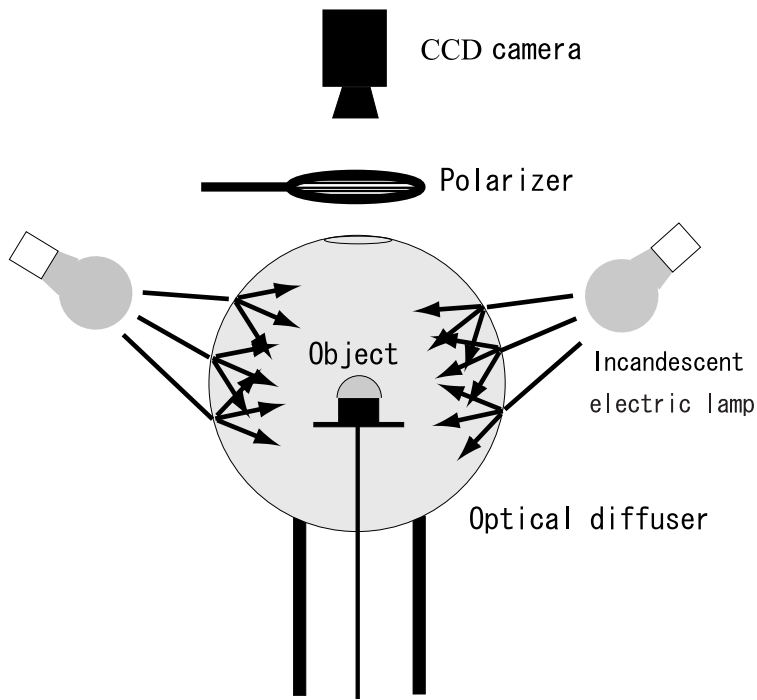
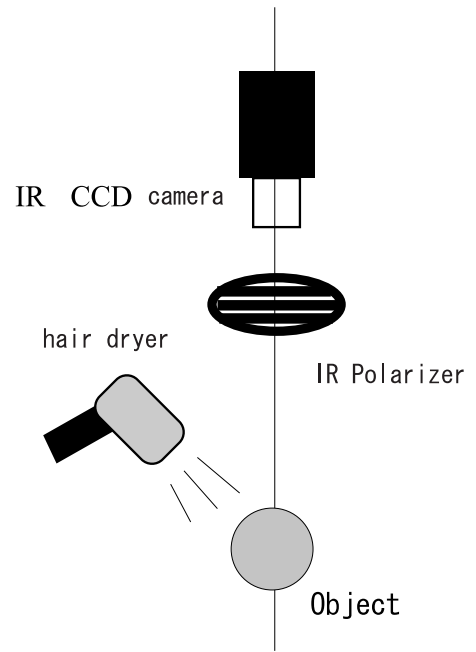


Fig. 5. Polarization degree of (a)infrared light ($n = 1.5$), and (b)visible light ($n = 1.5$)



(a) Apparatus for Visible Light



(b) Apparatus for Infrared Light

Fig. 6. Experimental setup

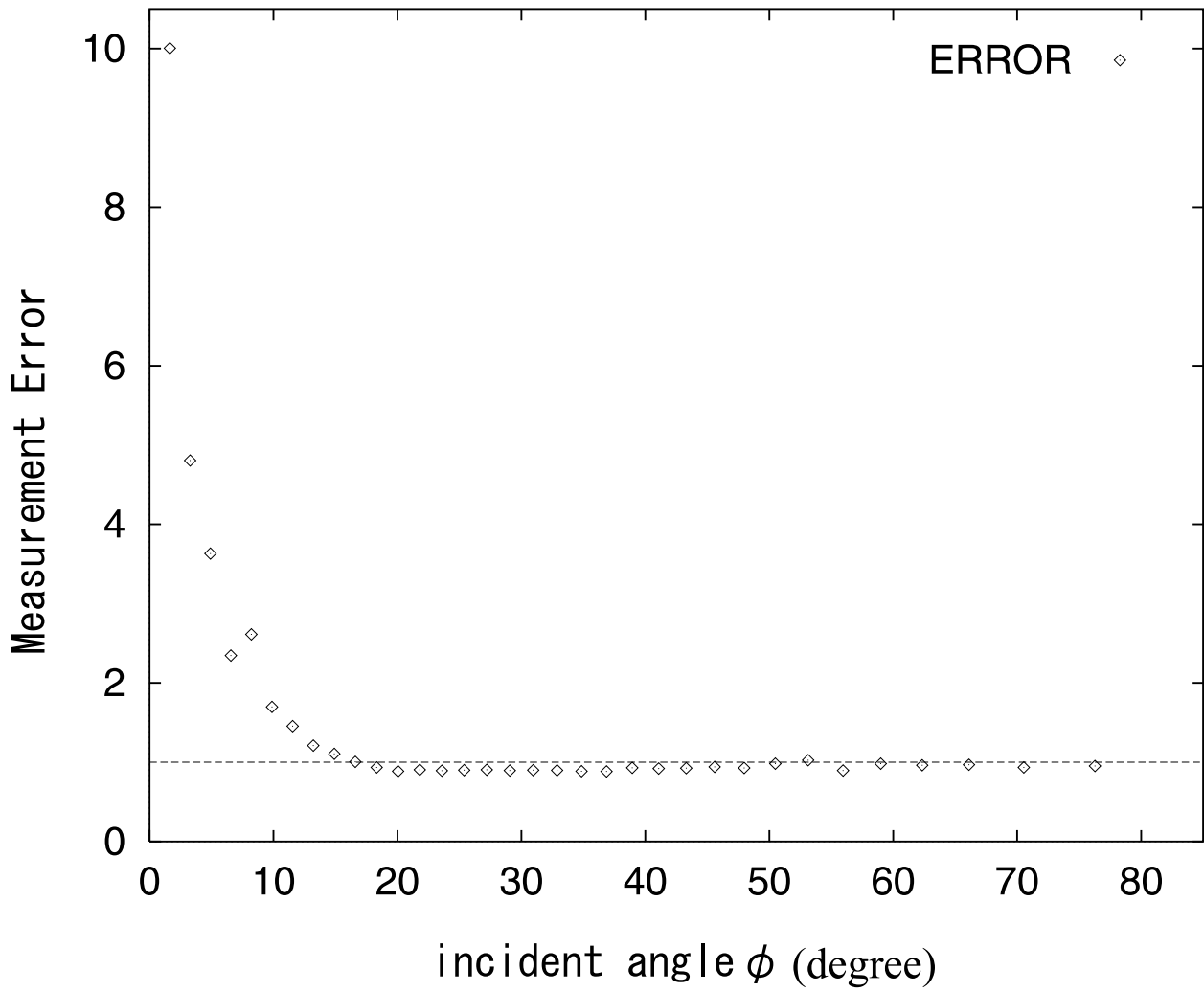
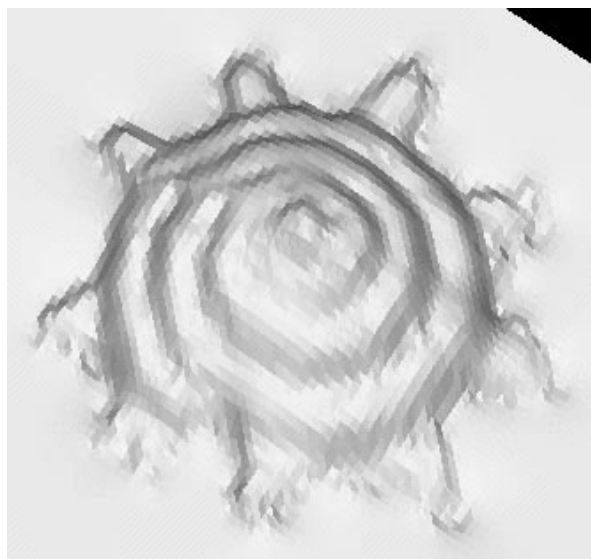
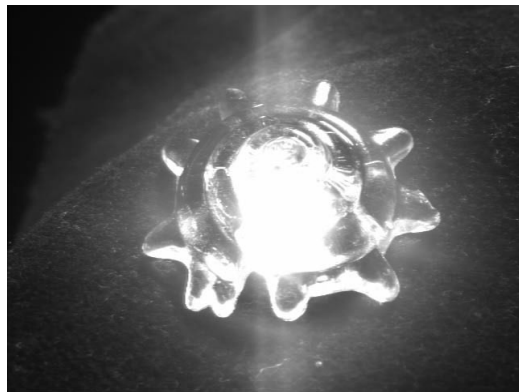


Fig. 7. Error characteristics of the spherical object



(a) Acrylic shellfish object

(b) Obtained shape

Fig. 8. The resulting shape of the shellfish-shaped object